Crystal Structure of α-1,4-Glucan Lyase, a Unique Glycoside Hydrolase Family Member with a Novel Catalytic Mechanism

Rozeboom, Henriëtte J.; Yu, Shukun; Madrid, Susan; Kalk, Kor H.; Zhang, Ran; Dijkstra, Bauke W.

Published in:
J. Biol. Chem.

DOI:
10.1074/jbc.M113.485896

Publication date:
2013

THE JOURNAL OF BIOLOGICAL CHEMISTRY VOL. 288, NO. 37, pp. 26764–26774, September 13, 2013

Crystal Structure of α-1,4-Glucan Lyase, a Unique Glycoside Hydrolase Family Member with a Novel Catalytic Mechanism

Received for publication, June 10, 2013, and in revised form, July 11, 2013 Published, JBC Papers in Press, July 31, 2013, DOI 10.1074/jbc.M113.485896

Henriëtte J. Rozeboom[‡], Shukun Yu[§1], Susan Madrid[§2], Kor H. Kalk[‡], Ran Zhang[¶], and Bauke W. Dijkstra[‡3]

From the [‡]Laboratory of Biophysical Chemistry, Groningen Biomolecular Sciences and Biotechnology Institute, University of Groningen, Nijenborgh 7, 9747 AG Groningen, The Netherlands, [§]Danisco Innovation, Danisco A/S, DK-1001 Copenhagen, Denmark, and the [¶]Department of Chemistry, University of British Columbia, Vancouver, British Columbia V6T 1Z1, Canada

Background: α-1,4-Glucan lyase (GLase) is a glycoside hydrolase family member that degrades starch via an elimination reaction.
Results: Crystal structures of GLase with covalently bound inhibitors show that the catalytic nucleophile can abstract the proton.
Conclusion: The nucleophile has a dual function, acting successively as nucleophile and base.
Significance: A single substitution converts a glycoside hydrolase into a lyase.

α-1,4-Glucan lyase (EC 4.2.2.13) from the red seaweed *Gracilariopsis lemaneiformis* cleaves α-1,4-glucosidic linkages in glycogen, starch, and malto-oligosaccharides, yielding the keto-monosaccharide 1,5-anhydro-D-fructose. The enzyme belongs to glycoside hydrolase family 31 (GH31) but degrades starch via an elimination reaction instead of hydrolysis. The crystal structure shows that the enzyme, like GH31 hydrolases, contains a $(\beta/\alpha)_8$-barrel catalytic domain with B and B′ subdomains, an N-terminal domain N, and the C-terminal domains C and D. The N-terminal domain N of the lyase was found to bind a trisaccharide. Complexes of the enzyme with acarbose and 1-dexoynojirimycin and two different covalent glycosyl-enzyme intermediates obtained with fluorinated sugar analogues show that, like GH31 hydrolases, the aspartic acid residues Asp^{553} and Asp^{665} are the catalytic nucleophile and acid, respectively. However, as a unique feature, the catalytic nucleophile is in a position to act also as a base that abstracts a proton from the C2 carbon atom of the covalently bound subsite −1 glucosyl residue, thus explaining the unique lyase activity of the enzyme. One Glu to Val mutation in the active site of the homologous α-glucosidase from *Sulfolobus solfataricus* resulted in a shift from hydrolytic to lyase activity, demonstrating that a subtle amino acid difference can promote lyase activity in a GH31 hydrolase.

Glycoside hydrolases (GHs)[4] are important biocatalysts that occur in nearly all forms of life, where they catalyze pivotal biological reactions including the hydrolytic degradation of oligo- and polysaccharides (1). On the basis of their primary structure and conserved sequence motifs, they have been grouped into >130 glycoside hydrolase families (2). However, nonhydrolytic enzymes, such as lyases, also exist and cleave glycosidic bonds. Polysaccharide lyases (EC 4.2.2.-) cleave the O-C4′ glycosidic bond by abstraction of the C5′ proton, followed by introduction of an alkene functionality between the C4′ and C5′ atoms (3). In contrast, α-1,4-glucan lyases (GLases; EC 4.2.2.13) cleave the glycosidic C1-O bond by abstraction of the C2 proton and formation of the enol form of anhydrofructose (Fig. 1) (4).

Based on sequence similarity and the cleavage of C1-O glycosidic bonds, GLases have been grouped as special members of glycoside hydrolase family 31 (GH31), instead of as members of a separate polysaccharide lyase family (5). They form GH31 subgroup 2, whereas subgroup 1 contains all known α-glucosidases, including such important enzymes as human lysosomal α-glucosidase, endoplasmic reticulum glucosidase II, and the digestive enzymes maltase-glucoamylase (MGAM) and sucrase-isomaltase. Subgroups 3 and 4 contain archaeal and bacterial α-xylosidases, respectively (6). Sequence alignment shows that GLases have 18–25% identity to the GH31 subgroup 1 α-glucosidases and less identity to the other subgroups. This alignment further revealed the existence of several signature sequences of subgroups 1 and 2 which include the motifs W*X*DM and W*X*GDN (5). The D in motif W*X*DM was shown to represent the catalytic nucleophile (7), whereas the D in W*X*GDN functions as the acid/base catalyst (8).

Mechanistic studies, based on kinetic isotope effects, suggested that the reaction catalyzed by GLases proceeds via two steps. In the first step a covalent GLase-substrate intermediate (the glycosylated GLase) is formed, which is similar to the first step of the double displacement reaction catalyzed by GH31 retaining glycoside hydrolases. For the second step, a *syn* elim-

This article contains supplemental Fig. S1.
The atomic coordinates and structure factors (codes 2X2H, 2X2I, 2X2J, 4AMW, and 4AMX) have been deposited in the Protein Data Bank (http://wwpdb.org/).

[1] To whom correspondence may be sent at the present address: Genencor, Danisco A/S, Edwin Rahrs Vej 38, DK-8220 Brabrand, Aarhus, Denmark. E-mail: shukun.yu@danisco.com.
[2] Present address: Danisco US Incorporation, Palo Alto, CA 94304.
[3] To whom correspondence may be addressed. Tel.: 31-50-363-4381/4378; Fax: 31-50-363-4800; E-mail: b.w.dijkstra@rug.nl.

[4] The abbreviations used are: GH, glycoside hydrolase; Acr, acarbose; Bis-Tris, bis(2-hydroxyethyl)iminotris(hydroxymethyl)methane; CBM, carbohydrate binding module; DNJ, 1-deoxynojirimicyn; 5FαGlcF, 5-fluoro-α-D-glucopyranosyl fluoride; 5FβIdoF, 5-fluoro-β-L-idopyranosyl fluoride; GLase, glucan lyase; MGAM, maltase-glucoamylase; PDB, Protein Data Bank; SBS, secondary carbohydrate binding site.

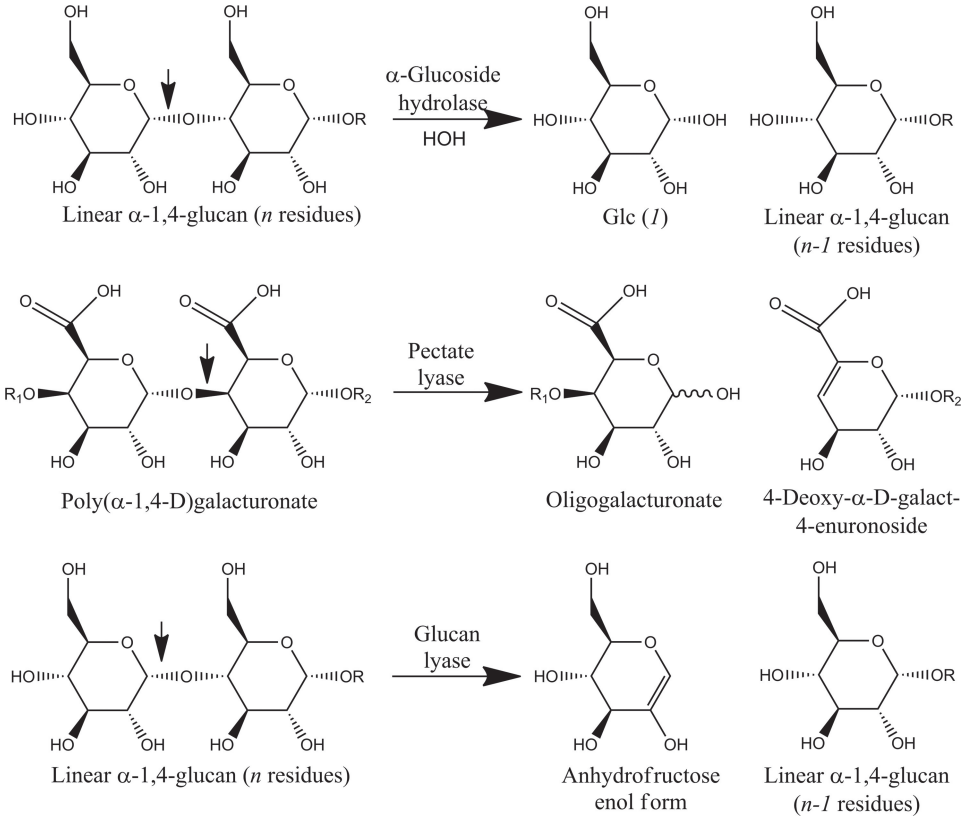

FIGURE 1. **Comparison of the three mechanisms of glycosidic bond breakage, exemplified, respectively, by glucoside hydrolases and two polysaccharide lyases.** For anhydrofructose the enol tautomer is shown, which is in equilibrium with the keto form as a result of enol-keto tautomerization (47).

ination of the GLase-substrate intermediate has been proposed, yielding an unsaturated sugar, 1,5-anhydrofructose, and the free enzyme GLase. Both the first and second reaction steps are supposed to proceed via oxocarbenium ion-like transition states (7, 9, 10). However, which residue abstracts the proton from the C2 atom of the sugar ring in the elimination reaction has remained unclear so far (9).

GLases are exo-enzymes that act from the nonreducing ends of the substrate. They degrade both malto-oligosaccharides and starch, suggesting that their active site comprises several glucosyl binding subsites (5, 11). Moreover, GLases and glycoside hydrolases share certain competitive inhibitors like 1-deoxynojirimycin and acarbose (5), with K_i values of 0.130 μM (9) and 0.002 μM (7), respectively. 1,5-Difluoroglycosides are also inhibitors of GLase (9). Such sugars are suitably activated at the anomeric carbon with an excellent leaving group. The C5-fluoro group increases the energy of the transition state, thus slowing down both reaction steps catalyzed by the enzyme, and therefore these fluorosugars can be used to label the catalytic nucleophile (12). It appeared that epimers of the parent fluorosugars inverted at C5 are more effective trapping reagents for GH38 α-mannosidase (13) and GH31 α-xylosidases (8, 14). Indeed, also for GLase, 5-fluoro-β-L-idopyranosyl fluoride (5FβIdoF) with a K_i of 28.3 $\pm$ 2.1 mM (7, 9) is more effective than 5-fluoro-α-D-glucopyranosyl fluoride (5FαGlcF), with an apparent dissociation constant K_i of 6.5 mM (9).

Here we report the x-ray structure of GLase from *Gracilariopsis lemaneiformis*, a lyase belonging to GH31, in its native form and in complexes with acarbose, 1-dexoynojirimycin, 5FβIdoF, and 5FαGlcF. We show that the catalytic nucleophile Asp^{553} functions as a nucleophile in the first step of the reaction forming the covalent enzyme-glycosyl intermediate but acts as a catalytic base in the second step, abstracting a proton from the C2 carbon atom of the covalently bound subsite −1 glucosyl residue. These results resolve the long time ambiguity on the nature of the proton abstracting residue (9, 10). Site-directed mutagenesis and enzymatic characterization of the archaeal α-glucosidase homologue MalA show that subtle changes are sufficient to confer lyase activity to a hydrolase.

MATERIALS AND METHODS

Expression and Purification of α-1,4-Glucan Lyase—The GLase gene was cloned from a DNA library using genomic DNA isolated from the red seaweed *G. lemaneiformis* (15) Expression cassettes were constructed, and intracellular expression of the GLase gene in the yeast *Hansenula polymorpha* was achieved as described previously (16). Four constructs were made representing full-length, N-terminally truncated, C-terminally truncated, and both N-and C-terminally truncated glucan lyases (Fig. 2). Purification of the recombinant glucan lyases was performed by anion exchange chromatography using Q-Sepharose FF with 20 mM Bis-Tris, pH 6.7, as buffer A, and buffer A containing 1.0 M NaCl as buffer B (17, 18). Further purification was achieved by a second anion exchange chromatography step using a Mono Q column and elution with a gradient of 0.28 – 0.32 M NaCl in 20 mM Bis-Tris, pH 6.7. Only the first fractions of the GLase peak from subsequent runs (with

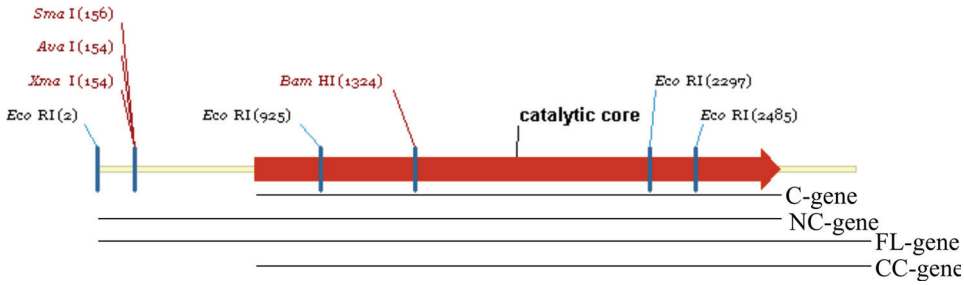

FIGURE 2. **Construction of four GLase expression cassettes.** FL-gene, coding for the full-length glucan lyase gene (1–1038); CC-gene, coding for the N-terminal truncated lyase (224–1038); NC-gene, coding for the C-terminal truncated lyase (1–938); and C-gene, coding for both N-and C-terminal truncated lyase (224–938). These constructs were used to transform *H. polymorpha* by electroporation.

TABLE 1

Data collection and structure refinement statistics

Values in parentheses are for the highest resolution shell.

	wt GLase	Acarbose soak	Deoxynojirimycin soak	5FIdoF soak	5FGlcF soak
Data collection					
Spacegroup	P1	$P2_1$	$P2_1$	P1	P1
Unit cell a, b, c (Å),	91.7, 96.6, 134.5	134.9, 91.9, 193.5	134.7, 91.8, 193.2	92.1, 97.3, 136.3	91.6, 97.0, 135.7
α, β, γ (°)	80.5, 83.3, 85.3	90.0, 99.4, 90.0	90.0, 99.3, 90.0	80.3, 83.3, 85.2	80.4, 83.1, 85.2
Resolution (Å)	2.06	2.60	2.35	1.90	2.10
No. of observations	3213515	1914405	1569071	663997	477958
No. of unique reflections	258096	322607	447794	340755	255868
R_{sym} (%)	6.7 (22.2)*	23.0 (64.0)	20.7 (69.0)	11.4 (49.6)	11.0 (47.7)
Completeness (%)	93.2 (76.4)	82.2 (79.3)	91.0 (85.2)	93.5 (94.1)	96.0 (92.3)
Mean I/σ (I)	13.8 (2.6)	3.4 (1.0)	4.3 (1.0)	5.3 (1.6)	5.1 (1.4)
Wilson *B* factor ($Å^2$)	20.3	42.0	33.5	16.2	24.8
Refinement					
R / Rfree (%)	16.8 / 21.4	23.4 / 31.9	23.4 / 29.1	20.7 /25.4	22.2 / 26.7
Monomers/asymmetric unit	4	4	4	4	4
No. of atoms					
Protein (chain A,B,C,D)	32660 (4100 residues)	32660	32660	32660	32660
Ligand	-	312	44	48	48
Waters	3766	836	1578	1427	923
Other atoms	130 (15 GOL, 9 OAc, 2 Cl^-)	42 (7 GOL)	70 (12 GOL, 4 Cl^-)	48 (8 GOL)	30 (5 GOL)
B factors ($Å^2$)					
main chain (A;B;C;D)	26.7; 36.4; 33.2; 28.8	39.1; 42.9; 37.4; 44.8	42.8; 48.1; 39.5; 53.8	17.0; 29.5; 29.1; 18.7	30.0; 41.0; 40.6; 31.6
ligand		38.1; 42.8; 41.6; 39.3	34.8; 36.5; 35.4; 36.1	28.0; 42.0; 38.9; 41.7	36.7; 44.7; 44.0; 47.6
ligand2		47.0; 66.8; 42.0; 72.2			
Waters	39.1	29.5	46.0	32.0	30.2
Geometry					
RMSD Bond lengths (Å)	0.007	0.009	0.010	0.014	0.011
RMSD Bond angles (°)	1.1	1.3	1.3	1.5	1.3
Ramachandran favored (%)	96.5	91.9	95.0	96.0	95.7
Ramachandran outliers (%)	0.2	0.5	0.2	0.2	0.1
Molprobity score	1.95	2.95	2.34	2.05	2.21
PDB accession code	2x2h	2x2i	2x2j	4amw	4amx

1 mg of protein/run) were pooled and concentrated to 9.7–17.0 mg protein ml^{-1}. Characterization of GLase with respect to its substrate specificity, N-terminal sequencing, and mass spectrometry analysis (MALDI-TOF) was as described before (17).

Crystallization and X-ray Data Collection—GLase crystals were obtained from hanging-drop experiments with 18–21% polyethylene glycol 8000 in 100 mM sodium acetate buffer (pH 5.0–5.2) as precipitant, using drops of 3 μl of protein solution (12.9 mg ml^{-1} in 20 mM Bis-Tris buffer, pH 6.7, 300 mM NaCl) and 3 μl of reservoir solution. Crystals grew in two different space groups (*P*1 and $P2_1$); both forms were used in the structure determinations (Table 1).

Before data collection, crystals were soaked for 15 s in a cryoprotectant solution, consisting of reservoir solution supplemented with 18% glycerol, directly followed by flash freezing. Native GLase data were collected at 100 K from a crystal belonging to space group *P*1 on beam line BW7A (DESY/EMBL, Hamburg, Germany). For inhibitor binding studies, crystals of space group $P2_1$ were soaked in a solution containing 15 mM acarbose (Serva Electrophoresis GmbH) or 125 mM 1-deoxynojirimycin (Sigma-Aldrich) for a few minutes. Data were collected in house at 110 K with a DIP2030H image plate detector using Cu-*Kα* radiation from a Bruker-AXS FR591 rotating anode generator equipped with Franks mirrors for the acarbose dataset or with Osmic mirrors for the 1-deoxynojirimycin dataset. Intensity data were processed using DENZO and SCALEPACK (19). For the 5-fluorosugar binding studies, crystals of space group *P*1 were soaked in solution containing 20

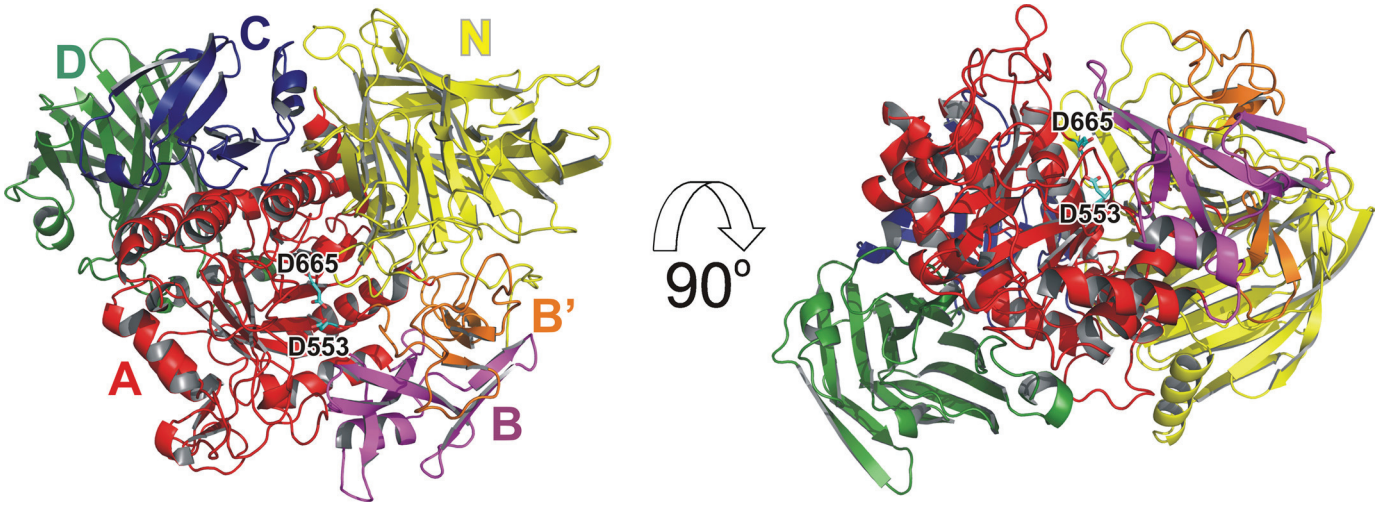

FIGURE 3. **Domain structure of GLase shown in two different orientations.** The individual domains are *colored* as indicated: N-terminal domain (domain N), *yellow*; central catalytic $(\beta/\alpha)_8$ barrel (domain A), *red*; subdomain B ($loop_{A\beta3}\rightarrow_{A\alpha3}$), *magenta*; subdomain B′ ($loop_{A\beta4}\rightarrow_{A\alpha4}$), *orange*; proximal C-terminal (domain C), *blue*; and the distal C-terminal domain (domain D), *green*. The catalytic residues are displayed as *sticks* in *cyan* and labeled as *D553* and *D665*.

mM 5FβIdoF for 30 min or 40 mM 5FαGlcF for 40 min. 5FαGlcF and 5FβIdoF were synthesized as described previously (20). Data were collected on beam line ID14-4 (ESRF, Grenoble, France) for 5FβIdoF and on beam line ID23-2 (ESRF) for 5FαGlcF. Intensity data were processed using iMosflm (21) and scaled using SCALA from the CCP4 suite (21) for 5FβIdoF, and with XDS (23) for 5FαGlcF. A summary of data collection statistics is given in Table 1.

Structure Determination and Refinement—The structure of native GLase was solved by molecular replacement with PHASER (24) using a model of the MalA structure (PDB code 2G3M (6)) made by the FFAS server (25) as a search model. In an iterative procedure, the phases were improved with NCSREF (22, 26) and the ARP/wARP procedure (27), combined with manual model improvement with COOT (28). Refinement with REFMAC5 (26) with TLS rigid body refinement (29) as last step, resulted in a final model comprising 4 protein molecules with 1025 residues each, 15 glycerol molecules, 9 acetate molecules, 2 chloride ions, and 3766 water molecules. Further details of the refinement are listed in Table 1. The electron density of the first 2 residues from all 4 GLase molecules is not visible.

The obtained structure of native GLase was used for molecular replacement with PHASER to solve the structures of GLase in complex with 1-deoxynojirimycin (GLase-DNJ), acarbose (GLase-Acr), 5FαGlcF, and 5FβIdoF. In the GLase-DNJ structure 1 deoxynojirimycin molecule was observed in the active site of each GLase molecule in the asymmetric unit. Continuous density in $F_o - F_c$ maps for 2 acarbose molecules/protein molecule was observed in the GLase-Acr crystal, one bound in the active site and one bound at a remote location. In the secondary substrate binding sites electron density is only visible for three of the four sugar residues; the reducing end glucose points into the solvent and is probably flexible. After rigid body refinement using REFMAC5 $2F_o - F_c$ and $F_o - F_c$ maps clearly showed density for 5FαGlc and 5FβIdo bound in the active sites. The inhibitor molecules were built with COOT, and the structures were refined using REFMAC5. No significant conformational changes are observed between native and ligand-bound enzymes. The Cα atoms of GLase superimpose with root mean square deviations of 0.3, 0.2, 0.3, and 0.2 Å for GLase-Acr, GLase-DNJ, 5FαGlc, and 5FβIdo, respectively. Analysis of the stereochemical quality of the models was done with MolProbity (30). Figures were prepared with PyMOL (Schrödinger).

Sulfolobus solfataricus α-Glucosidase (MalA) Mutagenesis, Expression, Purification, and Characterization—Wild type and mutant strains of MalA, with codon optimization for growth in *Escherichia coli*, were ordered from Sloning BioTechnology (Puchheim, Germany) and were inserted into the isopropyl-β-D-thiogalactopyranoside-inducible expression vector pET-24a which contains a kanamycin resistance marker and a C-terminal His_6 tag. For the construction of the Glu^{323}, mutant primers containing the mutation were introduced with the QuikChange Site-directed mutagenesis kit, using plasmid pET-24a-MalA-I213V/I249N/D251T (triple mutant) as the template. Successful mutagenesis was confirmed by nucleotide sequencing. Expression of the construct was achieved in *E. coli* BL21(DE3) cells grown in LB medium. All cultivation media contained 50 $\mu g\ ml^{-1}$ kanamycin. At an A_{600} of 0.5–0.7, the cells were induced with 1.0 mM isopropyl-β-D-thiogalactopyranoside for a few hours at 180 rpm and 37 °C. SDS-PAGE was performed to investigate protein expression. The cell pellets were resuspended and washed in 50 mM Tris-HCl, pH 8.0, with 100 mM NaCl and disrupted with a French press. After centrifugation, the resultant extract was partly purified by HisTrap HP (GE Healthcare) chromatography with an imidazole gradient in 20 mM Tris, pH 7.5. Further purification was achieved by gel filtration chromatography using a Superdex 200 column with 20 mM Tris, pH 7.5, and 0.2 M NaCl. α-Glucosidase activity was analyzed as in Ref. 6. Glucan lyase activity was assayed with the DNS reagent (31) and with *O*-ethylhydroxylamine at 21 °C (32). After the reaction of enzyme with maltose, the samples were incubated with *O*-ethylhydroxylamine/HCl at 21 °C for at least 2 h and then centrifuged at 13,000 rpm. The resulting oximes were separated on an ÄKTAmicro system (GE Healthcare) equipped with a Sephasil C18 analytical column (4 × 250 mm, 5 μm; GE Healthcare) with as mobile phase an increasing gradient of

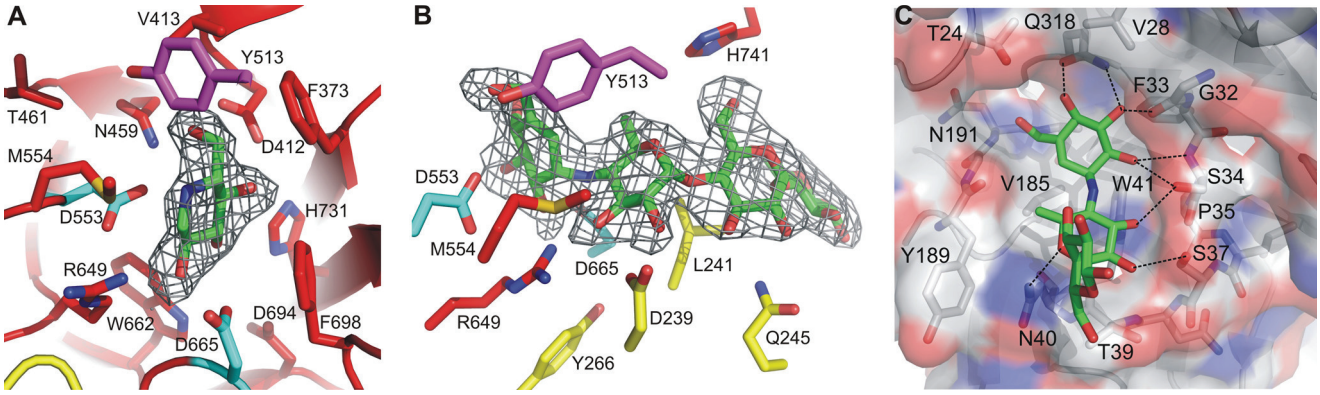

FIGURE 4. **The active site.** *A*, GLase in complex with 1-deoxynojirimicyn (GLase-DNJ) (*green*) bound in subsite −1 with $F_o - F_c$ omit electron density contoured at 3.0 σ. *B*, GLase in complex with acarbose (GLase-Acr) (*green*) bound in subsites −1, +1, +2, and +3 with $F_o - F_c$ omit electron density contoured at 3.0 σ. Further *color coding* of main chain and side chains are as in Fig. 3. For clarity, only side chains in *B* are shown. *C*, image of acarbose (*green*) bound in the putative starch binding site at the N-terminal domain N of GLase-Acr in *cpk colored stick* and *transparent surface* presentation.

acetonitrile (0–50%) in water, pumped at a flow rate of 0.3 ml/min. Detection was performed with a UV monitor at 207 nm. Pure anhydrofructose at different concentrations was used as a positive control.

RESULTS AND DISCUSSION

Overall Structure of α-1,4-Glucan Lyase—The structure of full-length *G. lemaneiformis* GLase missing 11 residues at its N terminus was solved by molecular replacement and refined against 2.06 Å resolution diffraction data to an *R*-factor of 0.168 (R_{free} = 0.214) with good stereochemistry (Table 1 and Fig. 3). Although the *P*1 unit cell contains 4 molecules of 1025 residues each, in solution the protein is monomeric, as shown by native PAGE analysis (33).

Each GLase molecule contains four major structural domains, which form a very compact structure with dimensions of 93 × 65 × 49 Å (Fig. 3). GLase starts with the N-terminal domain (domain N, residues 12–332) and continues with the catalytic A domain (residues 333–785). The A domain has a $(\beta/\alpha)_8$-barrel fold, with two inserted subdomains, B and B′. The structure is completed with the proximal and distal C-terminal domains (domain C, residues 784–879, and domain D, residues 880–1038, respectively). Domains N, C, and D are rich in β-sheets. The β-sheet content of GLase (28%) agrees with circular dichroism studies (34). Despite the presence of 15 cysteine residues in GLase none of them forms disulfide bonds.

The compactness of the GLase structure may explain its resistance to proteolytic cleavage. Only after prolonged reaction time, were proteinase K and subtilisin able to produce two fragments (34), with the higher molecular mass fragment starting at Ser^{175}, showing that the only site susceptible to these proteases is the surface loop ^{173}ASSG^{176} (marked *orange* in supplemental Fig. S1).

The GLase structure is very similar to the structures of the eight other structurally characterized GH31 family members, with DALI Z-scores over 30, despite root mean square deviation values >2.7 Å and sequence identities below 21%. These proteins are the N- and C-terminal catalytic subunits of human intestinal MGAM (NtMGAM; PDB code 2QLY (35), CtMGAM; PDB code 3TON (36)), human sucrase-isomaltase (PDB code 3LPO (37)), *Ruminococcus obeum* α-glucosidase (Ro-αG1; PDB code 3N04 (38)), *Sulfolobus solfataricus* α-glucoside hydrolase (MalA; PDB code 2G3M (6)), *Cellvibrio japonicus* α-xylosidase (CjXyl; PDB code 2XVG (14)) and α-transglucosylase (CjAgd; PDB code 4B9Y (39), and *E. coli* α-glycosidase (YicI; PDB code 1WE5 (7)). Most of the conserved residues are located in the A domain (supplemental Fig. S1), in agreement with its important substrate binding and catalytic function.

Domain N Contains a Secondary Carbohydrate Binding Site (SBS)—The large N-terminal domain folds into a double-layered twisted 19-strand β-supersandwich (Fig. 3). This fold belongs to the galactose-mutarotase-like superfamily and possibly functions as a carbohydrate binding domain in enzymes acting on saccharides (see the SCOP database (40)). The N domain contains loops that interact intimately with the catalytic domain and accommodate several invariant residues crucial for activity and active site architecture (supplemental Fig. S1). Among them are residues Gly^{212}, Glu^{215}, Asp^{239}, and Tyr^{266} from the N_I, N_{II}, and N_{III} motifs **G**LA**E**, YNV**D,** and PM**Y**YAAP, respectively (6) (supplemental Fig. S1). Residue Gly^{212} has main chain torsion angles disallowed for other amino acids (φ and ψ are 115° and 129°), nor is there space for a larger side chain. Residue Glu^{215} is hydrogen-bonded with one of its side chain oxygen atoms to the backbone amide of residue Tyr^{266}, of which the hydroxyl group, in turn, makes a hydrogen bond with the backbone amide of residue Asp^{665}, the catalytic acid. Residue Asp^{239} directly participates in substrate binding (see below). Thus, residues Gly^{212}, Glu^{215}, and Tyr^{266} appear important to stabilize the architecture of the active site in domain A.

Expression of full-length *G. lemaneiformis* GLase in *H. polymorpha* yielded an active glucan lyase missing 11 residues at the N terminus, as revealed by N-terminal amino acid sequencing. Nevertheless, its activity and substrate specificity were indiscernible from the wild type enzyme (15, 33), indicating that the 11 N-terminal residues were not essential for activity and expression in *H. polymorpha*. In contrast, no expression of variants with a larger N-terminal truncation (containing only residues 224–1038 or 224–938) was observed. Most likely no active enzyme is produced because these constructs lacked 2 of the 3 residues that stabilize the active site architecture.

GLase binds to raw starch (33), but amino acid sequence alignments with enzymes having carbohydrate binding modules (CBMs) did not reveal any similarity (5). The crystal structure of GLase-Acr revealed that GLase binds 2 acarbose molecules, 1 in the active site (see below) and the other to the N-terminal domain in a cleft between residues 32–37 and residues 189–191 (Fig. 4*C*). This latter acarbose is bound to the enzyme with its nonreducing end valienamine and dideoxyglucose units only, but not with its maltose part. Soaking experiments with the monosaccharide analog deoxynojirimycin (GLase-DNJ) and the fluorosugars 5FβIdoF and 5FαGlcF did not reveal any binding to the N domain of GLase, suggesting that minimally a α-1,4-linked glucose disaccharide is needed for recognition and binding by the N domain.

Several glycoside hydrolase families are known to have CBMs associated with a starch binding function. Domain N of GLase differs from these known CBMs in its amino acid sequence, size, and fold and its specificity for nonreducing end glucan disaccharide moieties. Aromatic amino acid are usually essential for the function of CBMs as they provide pi stacking interactions with the sugar rings (41), but as seen in Fig. 4*c*, residues Phe^{33} and Trp^{41} in GLase bind acarbose via Van der Waals interactions. This implies that this binding site should be regarded as a SBS (41). Sequence alignments of members of the GH31 family indicate that such SBSs exist in other algal glucan lyases, and a variant form may exist in fungal glucan lyases (4). Although these findings suggest that domain N of GLase contains a SBS, it is not conserved in other GH31 members. A possible reason could be that such a binding site is only advantageous for proteins that act on larger substrates such as glycogen and starch granules.

Domains C and D—The proximal C-terminal domain consists of an eight-stranded antiparallel β-sandwich with a 3_{10}-helix and a small α-helix (αC1) inserted after the first strand. It is packed between the N, A, and D domains (Fig. 3 and supplemental Fig. S1). The 6-residue 3_{10}-helix between βC5 and βC6, absent in other GH31 enzymes, is very well stabilized between the A and D domains.

The 159 C-terminal residues of GLase form domain D. Domain D is made up of a 12-stranded mostly antiparallel β-sandwich, consisting of two sheets of six strands, two α-helices after strands βD3 and βD9, and two 3_{10}-helices after strands βD1 and βD11. This domain has major interactions with domains C and A, especially via helices αD1 and αD2 (supplemental Fig. S1). Expression of a truncated GLase variant (1–938) missing 100 residues from the C terminus showed activity, although 10–20-fold decreased, indicating that the 100 C-terminal residues were not essential for activity and expression in *H. polymorpha*. Other GH31 members contain a similar D domain (see *e.g.* Ref. 42).

Domain A and the Active Site Structure—The catalytic domain A consists of a $(\beta/\alpha)_8$-barrel (TIM-barrel) with two additional helices, αA′ and Aα8′. The two additional domains, B (residues 462–530) and B′ (residues 556–615), are inserted after βA3 and βA4, respectively (Fig. 3 and supplemental Fig. S1). The secondary structure elements of subdomain B (a 3-stranded sheet and an α-helix) are the same as those in the other GH31 members NtMGAM, CtMGAM, Ro-αG1, sucrase-isomaltase, CjAgd, and MalA, but in GLase the sheet is longer and closer to the active site. An extra loop in subdomain B (residues 490–504) interacts with the N terminus and subdomain B′.

The active site of GLase is located at the C-terminal end of the $(\beta/\alpha)_8$-barrel of domain A. Residues from the loops following strands βA1, βA6, βA7, and βA8 shape the active site. Furthermore, loops from the N domain (243–262), the B domain (512–518), and B′ domain (559–590) make up the entrance to the active site (Fig. 3). The catalytic nucleophile Asp^{553} (7) is positioned at the end of strand βA4. The distance between the carboxylic acid oxygen atoms of residues Asp^{553} and Asp^{665} is 5.8 Å, which makes residue Asp^{665} the probable acid/base catalyst. This distance is similar to that found in retaining glycoside hydrolases, which is ~5.5 Å (43). In the structure of native GLase, 2 glycerol molecules from the cryoprotectant, known to often mimic sugar substrates, are bound in the active site.

The nucleophile Asp^{553} is hydrogen-bonded to residues Arg^{649}, Asn^{459}, the O_2 atom of a glycerol molecule, and 2 water molecules. The acid/base Asp^{665} has interactions with 3 water molecules and the O1 atom of the second glycerol molecule. The residues at the C termini of the β-sheets in the active site vicinity include Phe^{373}, Asp^{412}, Asn^{459}, Asp^{553}, Arg^{649}, Trp^{662}, Asp^{694}, and His^{731} from β-strands A1 to A8, respectively. Together with residues Trp^{551}, Met^{554}, Phe^{698}, Arg^{729}, and Tyr^{513}, they form subsite −1. The narrow entrance to the −1 subsite, creating a true pocket, is mainly formed by residues Phe^{373}, Tyr^{513}, Met^{554}, Arg^{649}, Asp^{665}, and Phe^{698}. The overall contours of the active site pocket of GLase are similar to those of the GH31 members MalA, NtMGAM, CtMGAM, sucrase-isomaltase, Ro-αG1, CjAgd, CjXyl, and YicI. However, amino acid substitutions of residues Phe^{373}, Val^{413}, Asn^{459}, Thr^{461}, and Tyr^{513} are observed (supplemental Fig. S1). Residue Tyr^{513} resides in subdomain B and is part of the extra loop, which is significantly different from a Trp residue that resides at the same site in other glycosidase GH31 members. Asn^{459} makes a hydrogen bond with the adjacent nucleophile Asp^{553}. This hydrogen bond is absent in the glycosidase members of GH31 where an Ile residue or a smaller Ser residue is present.

Binding of 1-Deoxynojirimycin and Acarbose—1-Deoxynojirimycin, a glucose analogue with a nitrogen instead of an oxygen atom in the pyranose ring, is bound in subsite −1 via hydrogen bonds (Fig. 4*A*). The hydroxyl groups of the 1-deoxynojirimycin make hydrogen bonds to residues Asp^{665}, Arg^{649}, His^{731}, Asp^{412}, Asp^{553}, Asn^{459}, and 2 water molecules. Residues Phe^{698}, Phe^{373}, Tyr^{513}, Trp^{551}, and Trp^{662} provide hydrophobic interactions.

Acarbose is bound to subsites −1 to +3 of GLase, with the valienamine residue binding to subsite −1, the 6-deoxyglucose residue to subsite +1, and the maltose subunit to subsites +2 and +3. Acarbose has a somewhat twisted conformation at the *N*-glycosidic bond, destroying the hydrogen bond between the sugar OH2 group in subsite −1 and the sugar OH3 group in subsite +1 as shown in Fig. 4*B*. Interactions involving the valienamine moiety of acarbose at subsite −1 are similar to those exhibited in the complex of 1-deoxynojirimycin and GLase. The nitrogen atom bound at C1, which mimics the glucosidic oxygen atom in α-1,4 linkages, is located between the

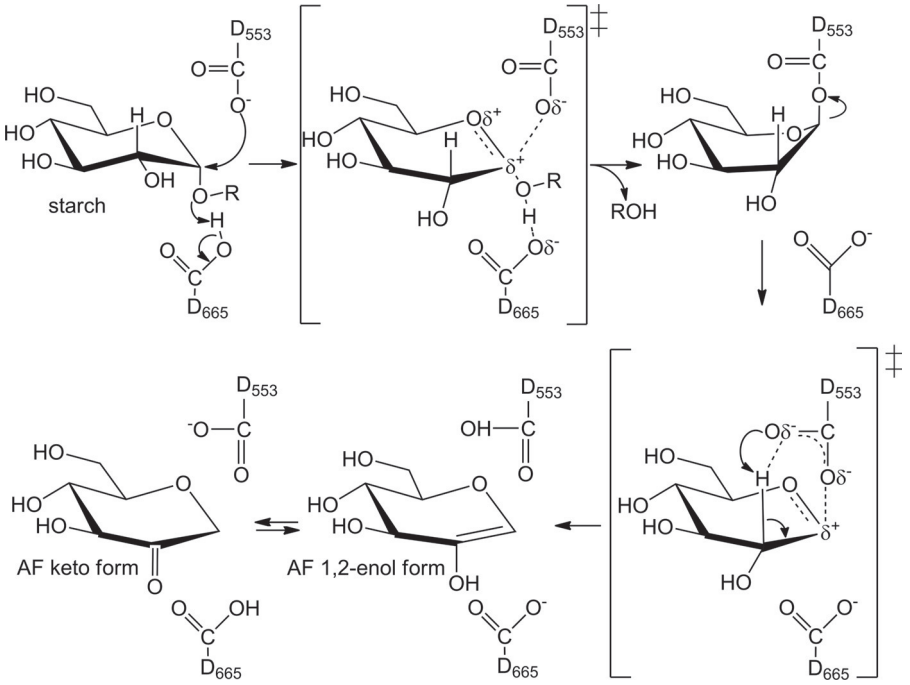

SCHEME 1. Proposed reaction mechanism of α-1,4-glucan lyase, modified from Yip and Withers (46).

two catalytic aspartates. Residue Asp^{665}-OD2 makes a hydrogen bond to the nitrogen atom, which would be an ideal orientation for protonation of a glucosidic oxygen. The binding of acarbose in subsite −1 is surprisingly similar to that of acarbose binding in NtMGAM, CtMGAM, and CjAgd.

Carbohydrate Binding Subsites +1, +2, and +3—For subsite +1, residues Arg^{649}, Asp^{239}, and Met^{553} interact with the OH3 group of the 6-deoxyglucose unit of acarbose. The OH2 group has hydrogen bonds with OD1 and OD2 of residue Asp^{239}. These hydrogen bonds compensate for the loss of the hydrogen bond between the OH2 group of the valienamine moiety and OH3 of the 6-deoxyglucose unit of acarbose. Residue Asp^{239} is conserved among GH31 members and always resides in the N-terminal domain. These interactions are essentially similar to those seen in the NtMGAM-acarbose complex. Mutating the equivalent residue of Asp^{239} in Ro-αG1 eliminated enzymatic activity, indicating its importance (38). In CjXyl and CjAgd the role of Asp^{239} is taken over by a Glu, present in the PA14 domain insert in the N-terminal domain of CjXyl and in the B′ domain of CjAgd (supplemental Fig. S1).

At the position matching the absent OH6 group of the dideoxyglucose unit enough space is available for a hydrogen bond of O6 to the backbone carbonyl of residue Tyr^{513} when an α-1,4-glucan is bound. The +1 sugar ring stacks against a hydrophobic cushion formed by the side chain of residue Tyr^{513} (Trp in the other GH31 family members) and residue Met^{554} (Met in other members, except for Ala in CjXyl, Leu in CjAgd, and Phe in YicI) (supplemental Fig. S1). A Trp residue at position 513 is strictly conserved in glycoside hydrolase members of family GH31 whereas in GLase it is replaced by a Tyr residue (4). The side chain of residue Leu^{241} is involved in hydrophobic interactions with the sugar rings at subsites +1, +2, and +3 (Fig. 4*B*). At subsite +2, residue Gln^{245} interacts with OH2 group of the glucose unit of acarbose and residue His^{741} on the opposite site of the groove interacts with OH6 group. At subsite +3, there are no interactions between the substrate and GLase (Fig. 4*B*).

The binding of acarbose completely shields subsite −1 from the solvent. Whereas residue Thr^{205} in NtMGAM and residue Gly^{89} in MalA allow space for entering water molecules used in the hydrolytic reaction, in GLase residue Leu^{241} blocks the entrance of water molecules (Fig. 4*A*). All hydrolases from family GH31 have a small or hydrophilic amino acid at this position, whereas the lyases have a larger hydrophobic amino acid (Leu or Met). Although sucrase-isomaltase also has a leucine at this position, it is located 2.5 Å away from Leu^{241}, thus creating more open +1 to +3 subsites. The α-transglucosylase, CjAgd, has also strong interactions with the acarbose, via a hydrophobic "sugar" clamp formed by 2 tyrosine residues (39). A similar clamp, made by 2 Trp residues, has also been observed in CjXyl (14). The binding of 1-deoxynojirimycin and acarbose, inhibitors of GLase, is illustrated in the second image of Scheme 1.

Substrate Specificity of GLase—Compared with the GH31 α-xylosidases YicI and CjXyl subsite −1 of GLase has more space enabling it to accommodate the hydroxymethyl group of α-1,4-glucans. Indeed, the double mutation C307I/F308D of YicI, designed to increase the space in the active site, converted the α-xylosidase into an α-glucosidase (44). Furthermore, the carbohydrate binding +2 subsite present in GLase allows the enzyme to act on longer α-1,4-glucans, in contrast to MalA, where subsite +2 is absent, and which consequently prefers the short disaccharide substrate maltose. Finally, the GH31 glucoside hydrolase Ro-αG1 prefers α-1,6- over α-1,4-linked substrates. This preference can be switched by a single W169Y mutation, which makes room for the 6-hydroxyl group of an α-1,4-linked glucose bound in subsite +1 (38). In GLase the equivalent residue is a phenylalanine (Phe^{373}), which also provides space for the 6-hydroxyl group of the +1 subsite sugar

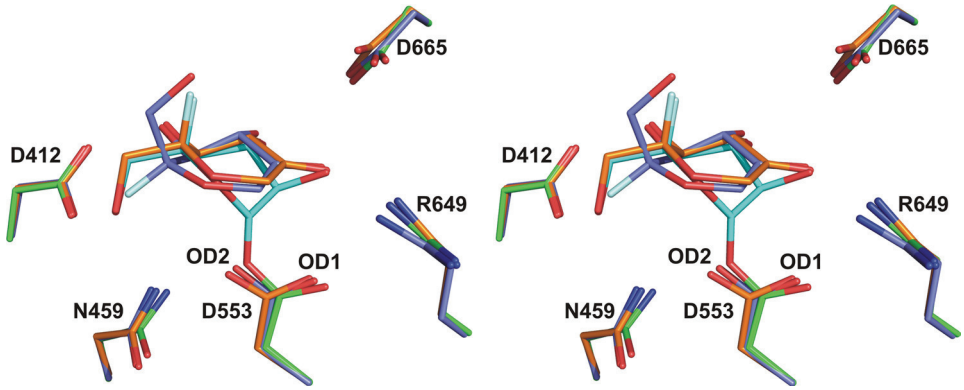

FIGURE 5. **Stereo view comparing the structures of 5Fαlc in the covalent intermediate (*green*/*cyan*) for monomer A, 5F-anhydrofructose/product (*orange*) in monomer D, and 5F-anhydrofructose/product in monomer of 5Fβldo (*slate blue*).**

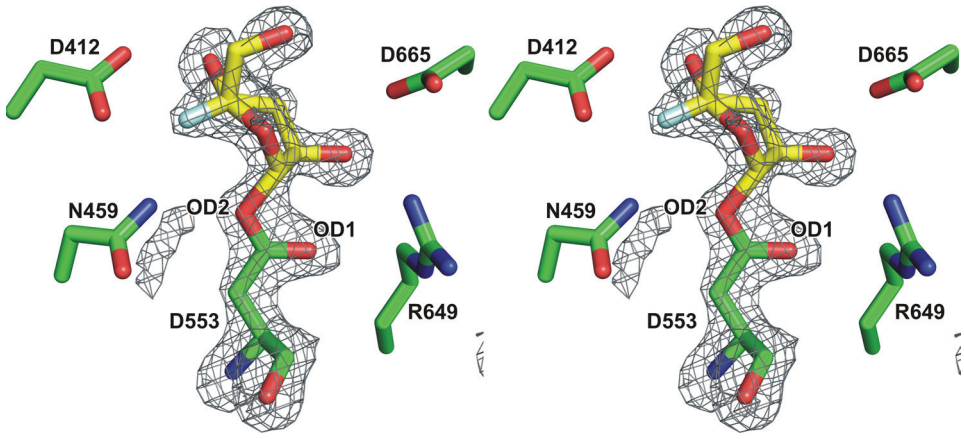

FIGURE 6. **Stereo view of simulated annealed omit electron density (50) of 5Fβldo (*yellow*) bound to Asp^{553}.** The density is shown for monomer A and is contoured at 3σ. For clarity, only the side chains are shown that have interactions with the fluorine atom and C2-OH hydroxyl group of the covalently bound sugar.

residue, in agreement with the strict preference of the enzyme for α-1,4-linked glucosides.

5FαGlcF and 5FβIdoF Bind Covalently to GLase—Soaking GLase crystals with the mechanism-based inhibitors 5FαGlcF and its C5-epimer 5FβIdoF revealed that these compounds were covalently bound via a β-glycosidic bond to Asp^{553} in three of the four monomers. However, in monomer D they have reacted because no electron density was present for a covalent bond to Asp^{553} and for a fluorine atom at C1 (Fig. 5). Indeed, the product 5F-anhydrofructose (or its C5 epimer) with a planar O5-C1-C2-O_2-C3 conformation could be fitted in the density present in the active site of monomer D. At the current resolution it is not possible to distinguish between the 1,2 enol and the keto forms of the product, but we have modeled the keto-5F-anhydrofructose (Fig. 5).

5FαGlc and 5Fβldo differ in the fluorine position at C5. In the glucose sugar the fluorine atom is positioned axially and has Van der Waals interactions with Phe^{698}. The glucose O6 hydroxyl is at hydrogen bonding distance to the OD2 atom of Asp^{412}. In contrast, the fluorine atom in the idose sugar is equatorially positioned and interacts with ND2 of Asn^{459}. The O6 of the idose sugar makes hydrogen bonds to a glycerol molecule and a water molecule. The different hydrogen bonding interactions of the idose sugar may explain the higher affinity and inhibitory power of this compound toward the enzyme (7).

The covalently bound fluorosugars have similar interactions as deoxynojirimycin except for their C1 and C2 atoms. Their conformations are distorted from the normal relaxed $^4C_1$ conformation (with an equatorial glycosidic bond) to a $^1S_3$ skew boat conformation, in which the glycosidic linkage is pseudo-axial (Figs. 5 and 6). The skew boat conformation allows a closer approach of the OD1 carboxyl oxygen of Asp^{553} to the C2 atom of the −1 glucose which would not be possible with the $^4C_1$ conformation of glucose (see third image of Scheme 1). This conformational distortion and the short distance between the carbonyl oxygen and the glucose C2 atom have important consequences for the catalytic mechanism (see below).

The 5Fαlc inhibitor is bound in the same conformation as in CjAgd (PDB code 4BA0) (39). In both structures the trapped 5Fαlc molecules are covalently linked to the OD2 of the nucleophiles. One remarkable difference in the −1 pocket is Asn^{459}, making a hydrogen bond to Asp^{553}, whereas in CjAgd this residue is a hydrophobic isoleucine as in all other glycosidase members of GH31.

Catalytic Mechanism—The crystal structures of GLase with various bound inhibitors indicate that the substrates bind with their nonreducing end in subsite −1 and extend toward the +*n* subsites. This binding mode is in agreement with biochemical experiments indicating that GLase degrades polysaccharides from the nonreducing end (4). 1-Deoxynojirimycin and acar-

bose are known to inhibit glucan hydrolases by mimicking the oxocarbenium ion-like transition state structure (7). In glucan lyase they may function in the same way because the first step in the reaction, the formation of a covalent enzyme-substrate intermediate, which proceeds via an oxocarbenium ion-like transition state, is the same for GH31 lyases and hydrolases (3, 5). In GLase, this first step is catalyzed by the Asp^{665} side chain, which acts as a general acid catalyst protonating the glycosidic oxygen of the scissile bond. Concomitantly, one of the carboxylate oxygen atoms of the nucleophile Asp^{553} attacks the C1 carbon of the substrate glycosyl residue bound at subsite −1, generating a covalently bound glycosyl-enzyme intermediate (Scheme 1 and Figs. 5 and 6). For the second reaction step, the deglycosylation, Lee *et al.* (9) have suggested an E1-like E2 concerted mechanism on the basis of kinetic isotope effect measurements. This means that, at the anomeric center, the glycosidic C-O bond is largely broken, generating a species with a highly developed oxocarbenium ion character, thereby acidifying the C2 proton and allowing its relatively facile removal late along the reaction coordinate. As suggested by the structures with covalently bound 5Fα-GlcF and 5Fβ-IdoF, the carbonyl oxygen atom of the nucleophile Asp^{553} is correctly positioned to abstract the proton from the sugar C2 carbon atom. Our proposed mechanism is similar to that of retaining glycosidases catalyzing the hydration of glycal substrates by *syn*-addition (the reverse of *syn*-elimination) of the C2 proton. In these enzymes the nucleophile is also assumed to participate in proton transfer (9, 45).

Both the acid/base catalyst Asp^{665} and the nucleophile Asp^{553} have, respectively, been assumed to have a dual role in proton abstraction by Yu *et al.* (4) and by Yip and Withers (46). Also, the possible existence of a separate base B^- in the active site (9) or a water molecule activated Asp^{665} (47) has been suggested. The acid catalyst Asp^{665} is positioned on the opposite side of the ring and consequently cannot abstract the proton from C2, nor is there a suitable water molecule situated. A separate base in the active site, able to abstract the proton, has not been observed. Arg^{649} makes a hydrogen bond to O_2 of the sugar and is also not correctly positioned. Asn^{459} is properly located but with 4.6 Å too far from C2 to abstract the proton. Instead, Asn^{459} donates a hydrogen bond to the adjacent carboxylate of nucleophile Asp^{553} (ester oxygen). In monomer D of the 5Fα-GlcF experiment this bond becomes shorter once the covalent intermediate has been released. Asn^{459} probably plays a key role in the second transition state stabilization by modulating the position and charge of the nucleophile.

Arg^{649} is strictly conserved in all GH31 enzymes. In GH31 hydrolase members this arginine has a salt bridge interaction with a conserved Glu at position 556 (supplemental Fig. S1), but in the GH31 lyases the residue equivalent to Glu^{556} is a Val or Thr. In GLase Arg^{649} makes hydrogen bonds with the OH3 atom of the glucose bound in subsite +1 and the OD1 atom of the catalytic nucleophile Asp^{553}. These interactions suggest that Arg^{649} is not only important for substrate recognition, but may also play a role in modulating the ionization state of Asp^{553}. The arginine side chain is in an apolar environment conferred by the side chains of Tyr^{266}, Trp^{662}, Met^{554}, and Val^{556}, which lowers the pK_a of its guanidinium group (48), enabling it to pick

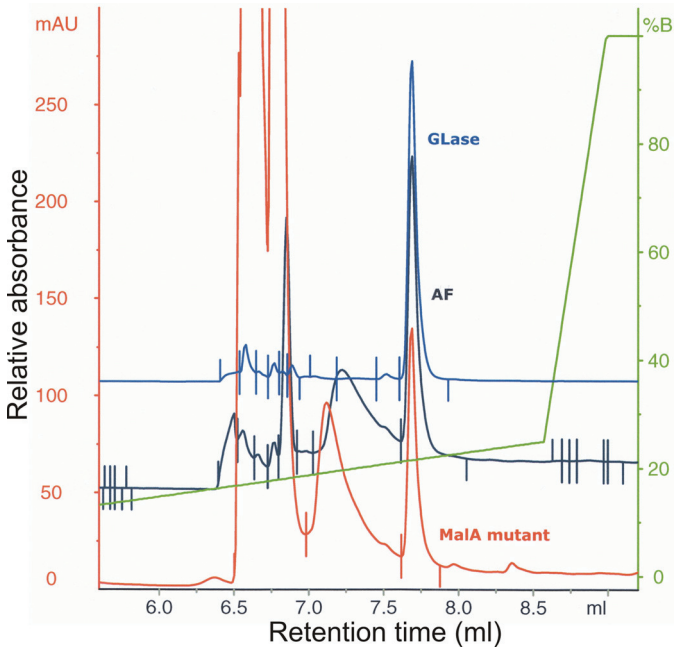

FIGURE 7. **Chromatogram of the reversed-phased HPLC analysis.** Indicated are the reaction products of GLase and MalA quadruple mutant on maltose, *AF* is the pure 1,5-anhydro-D-fructose. The sugars are derivatized with *O*-ethylhydroxylamine before being subjected to HPLC (32). Reaction time for the quadruple MalA mutant was 90 h; for wild type GLase, 30 min at 21 °C. Calculations based on peak area of the HPLC analysis indicate that the MalA mutant has an activity of 0.029 nmol of AF min^{-1} mg^{-1} and wild type GLase 2.9 μmol of AF min^{-1} mg^{-1}. The quadruple mutant has 0.001% (~100,000 times lower) activity of the wild type GLase at 21 °C. The retention time of the derivatized AF is 7.69 ml. Further detailed kinetic characterization of the MalA mutants remains to be done.

up the proton abstracted from the sugar by Asp^{553}. Subsequently, this proton can be relayed to the solvent via Asp^{239} or to the catalytic acid Asp^{665} for the next catalytic cycle after the product has left the active site. Indeed, in monomer D of the 5Fβ-IdoF experiment the Arg^{649} guanidinium group has rotated by approximately 25° toward D553 OD1 thereby reducing the distance to D553 OD1 from 3.4 to 2.9 Å. This suggests that residue 556 (being either a Glu or a Val) is a major determinant of the hydrolase *versus* lyase reaction specificity of GH31 enzymes.

Shift of α-Glucoside Hydrolase Activity to Lyase Activity—As argued above, the nature of the amino acid residue at position 556 (Val/Thr *versus* Glu) is very important for the reaction and product specificity of GH31 enzymes. Support for this notion comes from kinetic studies of the GH31 α-glucosidase from *Schizosaccharomyces pombe* (49), which showed that mutation of the residue equivalent to Val^{556} of GLase (E484A) eliminated its hydrolase activity, but that the enzyme retained 5% hydration activity on D-glucal to produce 2-deoxy-D-glucose by protonation at C2 (the reverse reaction of GLase). To demonstrate the importance of the residue at position 556 for lyase activity, an E323V mutation (Val^{556} in GLase) was introduced into the archaeal GH31 α-glucosidase MalA. We used a triple mutant of MalA (I213V/I249N/D251T; GLase $V^{413}N^{459}T^{461}$), which already had greatly reduced hydrolase activity but was unable to form anhydrofructose. The specific activity of the partially purified triple mutant was 0.012 ± 0.004 μmol/min/mg of protein, compared with 0.362 ± 0.005 μmol/min/mg of the par-

tially purified wild type MalA. For the quadruple MalA mutant (I213V/I249N/D251T/E323V) the expressed protein formed (soluble) aggregates after HisTrap purification. By storing the protein at 22 °C and removing the imidazole, a MalA protein of about 450 kDa could be resolved by gel filtration, which is similar to the molecular mass described previously (6). The quadruple mutant showed detectable lyase activity at high protein concentration and after prolonged reaction time (Fig. 7), whereas it had completely lost glucosidase activity. Thus, the E323V mutation in MalA shifts the reaction toward lyase activity, demonstrating the importance of position 323 (556) for hydrolase/lyase activity, likely by modulating the conformation of the fully conserved arginine in the active site. Evolving MalA into a genuine lyase with a K_{cat} similar to GLase will require further mutational studies.

Structures of all four subgroups of GH31 (6) have now been determined. Intriguingly, whereas the three-dimensional structures and catalytic site architectures are very similar and the essential catalytic residues are fully conserved, GLases show very different reaction specificity compared with the GH31 glucan hydrolases. Our results show that indeed the first step of the reaction, the formation of a covalent enzyme-substrate intermediate, is conserved. However, the glucosyl intermediate is not hydrolyzed like in the GH31 hydrolases, but a subtle change, a Val instead of a Glu at position 556, in the active site now promotes a lyase reaction. As a consequence the nucleophile in the lyase has acquired a dual function and can also act as a base, abstracting the proton from the C2 atom of the −1 glucose residue. Nature therefore has chosen a simple way in evolving new enzyme activities through clever changes at a localized area in the active site environment.

Acknowledgments—We thank K. Larsen and C. P. Walter for excellent technical assistance with expression and characterization of the glucan lyase and Dr. H. Pedersen for help with the fermentation of the Hansenula strain. We thank the staff scientists and local contacts at beam lines ID14-4 and ID23-2 at the ESRF, Grenoble, France, and BW7A at the EMBL-Hamburg outstation (DESY), Germany, for support during data collection.

REFERENCES

1. Henrissat, B., Sulzenbacher, G., and Bourne, Y. (2008) Glycosyltransferases, glycoside hydrolases: surprise, surprise! *Curr. Opin. Struct. Biol.* **18,** 527–533
2. Cantarel, B. L., Coutinho, P. M., Rancurel, C., Bernard, T., Lombard, V., and Henrissat, B. (2009) The carbohydrate-active enzymes database (CAZy): an expert resource for glycogenomics. *Nucleic Acids Res.* **37,** D233–238
3. Lombard, V., Bernard, T., Rancurel, C., Brumer, H., Coutinho, P. M., and Henrissat, B. (2010) A hierarchical classification of polysaccharide lyases for glycogenomics. *Biochem. J.* **432,** 437–444
4. Yu, S., and Marcussen, J. (1999) in *Recent Advances in Carbohydrate Bioengineering* (Gilbert, H. J., Davies, G., Henrissat, B., and Svensson, B., eds) pp. 243–250, Royal Society of Chemistry Press, London, UK
5. Yu, S., Bojsen, K., Svensson, B., and Marcussen, J. (1999) α-1,4-Glucan lyases producing 1,5-anhydro-D-fructose from starch and glycogen have sequence similarity to α-glucosidases. *Biochim. Biophys. Acta* **1433,** 1–15
6. Ernst, H. A., Lo Leggio, L., Willemoës, M., Leonard, G., Blum, P., and Larsen, S. (2006) Structure of the *Sulfolobus solfataricus* α-glucosidase: implications for domain conservation and substrate recognition in GH31. *J. Mol. Biol.* **358,** 1106–1124
7. Lee, S. S., Yu, S., and Withers, S. G. (2002) α-1,4-Glucan lyase performs a *trans*-elimination via a nucleophilic displacement followed by a *syn*-elimination. *J. Am. Chem. Soc.* **124,** 4948–4949
8. Lovering, A. L., Lee, S. S., Kim, Y. W., Withers, S. G., and Strynadka, N. C. (2005) Mechanistic and structural analysis of a family 31 α-glycosidase and its glycosyl-enzyme intermediate. *J. Biol. Chem.* **280,** 2105–2115
9. Lee, S. S., Yu, S., and Withers, S. G. (2003) Detailed dissection of a new mechanism for glycoside cleavage: α-1,4-glucan lyase. *Biochemistry* **42,** 13081–13090
10. Lee, S. S., Yu, S., and Withers, S. G. (2005) Mechanism of action of exo-acting α-1,4-glucan lyase: a glycoside hydrolase family 31 enzyme. *Biologia Bratislava* **60,** 137–148
11. Yoshinaga, K., Fujisue, M., Abe, J., Hanashiro, I., Takeda, Y., Muroya, K., and Hizukuri, S. (1999) Characterization of exo-(1,4)-α glucan lyase from red alga *Gracilaria chorda*: activation, inactivation and the kinetic properties of the enzyme. *Biochim. Biophys. Acta* **1472,** 447–454
12. McCarter, J. D., and Withers, S. G. (1996) Unequivocal identification of Asp-214 as the catalytic nucleophile of *Saccharomyces cerevisiae* α-glucosidase using 5-fluoro glycosyl fluorides. *J. Biol. Chem.* **271,** 6889–6894
13. Numao, S., Kuntz, D. A., Withers, S. G., and Rose, D. R. (2003) Insights into the mechanism of *Drosophila melanogaster* Golgi α-mannosidase II through the structural analysis of covalent reaction intermediates. *J. Biol. Chem.* **278,** 48074–48083
14. Larsbrink, J., Izumi, A., Ibatullin, F. M., Nakhai, A., Gilbert, H. J., Davies, G. J., and Brumer, H. (2011) Structural and enzymatic characterization of a glycoside hydrolase family 31 α-xylosidase from *Cellvibrio japonicus* involved in xyloglucan saccharification. *Biochem. J.* **436,** 567–580
15. Bojsen, K., Yu, S., Kragh, K. M., and Marcussen, J. (1999) A group of α-1,4-glucan lyases and their genes from the red alga *Gracilariopsis lemaneiformis*: purification, cloning, and heterologous expression. *Biochim. Biophys. Acta* **1430,** 396–402
16. Cook, M. W., and Thygesen, H. V. (2003) Safety evaluation of a hexose oxidase expressed in *Hansenula polymorpha*. *Food Chem. Toxicol.* **41,** 523–529
17. Yu, S., Ahmad, T., Kenne, L., and Pedersén, M. (1995) α-1,4-Glucan lyase, a new class of starch glycogen-degrading enzyme. 3. Substrate specificity, mode of action, and cleavage mechanism. *Biochim. Biophys. Acta* **1244,** 1–9
18. Yu, S., Christensen, T. M., Kragh, K. M., Bojsen, K., and Marcussen, J. (1997) Efficient purification, characterization and partial amino acid sequencing of two α-1,4-glucan lyases from fungi. *Biochim. Biophys. Acta* **1339,** 311–320
19. Otwinowski, Z., and Minor, W. (1997) Processing of x-ray diffraction data collected in oscillation mode. *Methods Enzymol.* **276,** 307–326
20. McCarter, J. D., and Withers, S. G. (1996) 5-Fluoro glycosides: a new class of mechanism-based inhibitors of both α- and β-glucosidases. *J. Am. Chem. Soc.* **118,** 241–242
21. Battye, T. G., Kontogiannis, L., Johnson, O., Powell, H. R., and Leslie, A. G. (2011) iMosflm: a new graphical interface for diffraction-image processing with MOSFLM. *Acta Crystallogr. D* **67,** 271–281
22. Winn, M. D., Ballard, C. C., Cowtan, K. D., Dodson, E. J., Emsley, P., Evans, P. R., Keegan, R. M., Krissinel, E. B., Leslie, A. G., McCoy, A., McNicholas, S. J., Murshudov, G. N., Pannu, N. S., Potterton, E. A., Powell, H. R., Read, R. J., Vagin, A., and Wilson, K. S. (2011) Overview of the CCP4 suite and current developments. *Acta Crystallogr. D* **67,** 235–242
23. Kabsch, W. (2010) XDS. *Acta Crystallogr. D* **66,** 125–132
24. McCoy, A. J., Grosse-Kunstleve, R. W., Adams, P. D., Winn, M. D., Storoni, L. C., and Read, R. J. (2007) PHASER crystallographic software. *J. Appl. Crystallogr.* **40,** 658–674
25. Jaroszewski, L., Rychlewski, L., Li, Z. W., Li, W. Z., and Godzik, A. (2005) FFAS03: a server for profile-profile sequence alignments. *Res. Nucleic Acids Res.* **33,** W284–288
26. Murshudov, G. N., Skubák, P., Lebedev, A. A., Pannu, N. S., Steiner, R. A., Nicholls, R. A., Winn, M. D., Long, F., and Vagin, A. A. (2011) REFMAC5 for the refinement of macromolecular crystal structures. *Acta Crystallogr. D* **67,** 355–367
27. Langer, G., Cohen, S. X., Lamzin, V. S., and Perrakis, A. (2008) Automated

macromolecular model building for x-ray crystallography using ARP/wARP version 7. *Nat. Protoc.* **3,** 1171–1179
28. Emsley, P., Lohkamp, B., Scott, W. G., and Cowtan, K. (2010) Features and development of COOT. *Acta Crystallogr. D* **66,** 486–501
29. Painter, J., and Merritt, E. A. (2006) TLSMD web server for the generation of multi-group TLS models. *J. Appl. Crystallogr.* **39,** 109–111
30. Chen, V. B., Arendall, W. B., 3rd, Headd, J. J., Keedy, D. A., Immormino, R. M., Kapral, G. J., Murray, L. W., Richardson, J. S., and Richardson, D. C. (2010) MolProbity: all-atom structure validation for macromolecular crystallography. *Acta Crystallogr. D* **66,** 12–21
31. Yu, S., Olsen, C. E., and Marcussen, J. (1998) Methods for the assay of 1,5-anhydro-D-fructose and α-1,4-glucan lyase. *Carbohydr. Res.* **305,** 73–82
32. Hirano, K., Ziak, M., Kamoshita, K., Sukenaga, Y., Kametani, S., Shiga, Y., Roth, J., and Akanuma, H. (2000) *N*-Linked oligosaccharide-processing enzyme glucosidase II produces 1,5-anhydrofructose as a side product. *Glycobiology* **10,** 1283–1289
33. Yu, S., Kenne, L., and Pedersén, M. (1993) α-1,4-Glucan lyase, a new class of starch glycogen-degrading enzyme. 1. Efficient purification and characterization from red seaweeds. *Biochim. Biophys. Acta* **1156,** 313–320
34. Ernst, H. A., Leggio, L. L., Yu, S., Finnie, C., Svensson, B., and Larsen, L. (2005) Probing the structure of glucan lyases by sequence analysis, circular dichroism and proteolysis. *Biologia Bratislava* **60,** 149–159
35. Sim, L., Quezada-Calvillo, R., Sterchi, E. E., Nichols, B. L., and Rose, D. R. (2008) Human intestinal maltase-glucoamylase: crystal structure of the N-terminal catalytic subunit and basis of inhibition and substrate specificity. *J. Mol. Biol.* **375,** 782–792
36. Ren, L., Qin, X., Cao, X., Wang, L., Bai, F., Bai, G., and Shen, Y. (2011) Structural insight into substrate specificity of human intestinal maltase-glucoamylase. *Protein Cell* **2,** 827–836
37. Sim, L., Willemsma, C., Mohan, S., Naim, H. Y., Pinto, B. M., and Rose, D. R. (2010) Structural basis for substrate selectivity in human maltase-glucoamylase and sucrase-isomaltase N-terminal domains. *J. Biol. Chem.* **285,** 17763–17770
38. Tan, K., Tesar, C., Wilton, R., Keigher, L., Babnigg, G., and Joachimiak, A. (2010) Novel α-glucosidase from human gut microbiome: substrate specificities and their switch. *FASEB J.* **24,** 3939–3949
39. Larsbrink, J., Izumi, A., Hemsworth, G. R., Davies, G. J., and Brumer, H. (2012) Structural enzymology of *Cellvibrio japonicus* Agd31B protein reveals α-transglucosylase activity in glycoside hydrolase family 31. *J. Biol. Chem.* **287,** 43288–43299
40. Murzin, A. G., Brenner, S. E., Hubbard, T., and Chothia, C. (1995) SCOP: a structural classification of proteins database for the investigation of sequences and structures. *J. Mol. Biol.* **247,** 536–540
41. Cuyvers, S., Dornez, E., Delcour, J. A., and Courtin, C. M. (2012) Occurrence and functional significance of secondary carbohydrate binding sites in glycoside hydrolases. *Crit. Rev. Biotechnol.* **32,** 93–107
42. Nakai, H., Ito, T., Tanizawa, S., Matsubara, K., Yamamoto, T., Okuyama, M., Mori, H., Chiba, S., Sano, Y., and Kimura, A. (2006) Plant α-glucosidase: molecular analysis of rice α-glucosidase and degradation mechanism of starch granules in germination stage. *J. Appl. Glycosci.* **53,** 137–142
43. McCarter, J. D., and Withers, S. G. (1994) Mechanisms of enzymatic glycoside hydrolysis. *Curr. Opin. Struct. Biol.* **4,** 885–892
44. Okuyama, M., Kaneko, A., Mori, H., Chiba, S., and Kimura, A. (2006) Structural elements to convert *Escherichia coli* α-xylosidase (YicI) into α-glucosidase. *FEBS Lett.* **580,** 2707–2711
45. Trincone, A., Pagnotta, E., Rossi, M., Mazzone, M., and Moracci, M. (2001) Enzymatic synthesis of 2-deoxy-β-glucosides and stereochemistry of β-glycosidase from *Sulfolobus solfataricus* on glucal. *Tetrahedron Asym.* **12,** 2783–2787
46. Yip, V. L., and Withers, S. G. (2006) Breakdown of oligosaccharides by the process of elimination. *Curr. Opin. Chem. Biol.* **10,** 147–155
47. Yu, S. (2008) The anhydrofructose pathway of glycogen catabolism. *IUBMB Life* **60,** 798–809
48. Guillén Schlippe, Y. V., and Hedstrom, L. (2005) A twisted base? The role of arginine in enzyme-catalyzed proton abstractions. *Arch. Biochem. Biophys.* **433,** 266–278
49. Okuyama, M., Okuno, A., Shimizu, N., Mori, H., Kimura, A., and Chiba, S. (2001) Carboxyl group of residue Asp647 as possible proton donor in catalytic reaction of α-glucosidase from *Schizosaccharomyces pombe*. *Eur. J. Biochem.* **268,** 2270–2280
50. Adams, P. D., Afonine, P. V., Bunkóczi, G., Chen, V. B., Davis, I. W., Echols, N., Headd, J. J., Hung, L. W., Kapral, G. J., Grosse-Kunstleve, R. W., McCoy, A. J., Moriarty, N. W., Oeffner, R., Read, R. J., Richardson, D. C., Richardson, J. S., Terwilliger, T. C., and Zwart, P. H. (2010) PHENIX: a comprehensive Python-based system for macromolecular structure solution. *Acta Crystallogr. D* **66,** 213–221